Pharm Res (2014) 31:382–393
DOI 10.1007/s11095-013-1167-4

RESEARCH PAPER

Impact of Different Vehicles for Laser-Assisted Drug Permeation *via* Skin: Full-Surface *versus* Fractional Ablation

Woan-Ruoh Lee • Shing-Chuan Shen • Ibrahim A. Aljuffali • Yi-Ching Li • Jia-You Fang

Received: 25 April 2013 / Accepted: 28 July 2013 / Published online: 11 September 2013

ABSTRACT

Purpose This study aimed to assess impact of different vehicles for laser-assisted skin drug delivery. We also tried to uncover the mechanisms by which different vehicles affect laser-aided skin permeation.

Methods Full-surface ablative (conventional) and fractional lasers were used to irradiate nude mouse skin. Imiquimod and 5-aminolevulinic acid (ALA) were used as lipophilic and hydrophilic permeants. Vehicles employed included water with 40% polyethylene glycol 400 (PEG 400), propylene glycol (PG), and ethanol. Lipid nanoparticles were also utilized as carriers.

Results *In vitro* permeation profiles showed improvement in imiquimod flux with conventional laser (2.5 J/cm^2) producing a 12-, 9-, and 5-fold increase when loading imiquimod in 40% PEG400, PG, and ethanol, respectively, as compared with intact skin. Nanoparticulate delivery by laser produced a 6-fold enhancement in permeation. Fractional laser produced less enhancement of imiquimod delivery than conventional laser. Laser exposure increased follicular imiquimod accumulation from 0.80 to 5.81 μg/cm^2. ALA permeation from aqueous buffer, PEG 400, and PG with conventional laser treatment was 641-, 445-, and 104-fold superior to passive control. *In vivo* skin deposition of topically applied ALA examined by confocal microscopy indicated the same trend as the *in vitro* experiment, with aqueous buffer showing the greatest proporphyllin IX signaling. Diffusion of cosolvent molecules into ablated skin and drug partitioning from vehicle to skin are two predominant factors controlling laser-assisted delivery. In contrast to conventional laser, lateral drug diffusion was anticipated for fractional laser.

Conclusions Our results suggest that different drug delivery vehicles substantially influence drug penetration enhanced by lasers.

KEY WORDS 5-aminolevulinic acid · ablative laser · imiquimod · nanoparticle · vehicle

INTRODUCTION

Topical/transdermal delivery is a method for transferring drugs into the body *via* skin. However, because the stratum corneum (SC) functions as a permeation barrier, only a

W.-R. Lee • S.-C. Shen
Graduate Institute of Medical Sciences, Taipei Medical University
Taipei, Taiwan

W.-R. Lee
Department of Dermatology, Taipei Medical University
Shuang Ho Hospital, New Taipei City, Taiwan

I. A. Aljuffali
Department of Pharmaceutics, College of Pharmacy
King Saud University Riyadh, Saudi Arabia

Y.-C. Li • J.-Y. Fang (✉)
Pharmaceutics Laboratory, Graduate Institute of Natural Products
Chang Gung University, 259 Wen-Hwa 1st Road
Kweishan, Taoyuan 333, Taiwan
e-mail: fajy@mail.cgu.edu.tw

Y.-C. Li
Chinese Herbal Medicine Research Team, Healthy Aging Research Center
Chang Gung University, Kweishan, Taoyuan, Taiwan

J.-Y. Fang
Chinese Medicine Research and Development Center
China Medical University Hospital, Taichung, Taiwan

J.-Y. Fang
Research Center for Industry of Human Ecology
Chang Gung University of Science and Technology
Kweishan, Taoyuan, Taiwan

limited range of drugs are clinically available through skin delivery systems. A number of strategies are currently employed to overcome the barrier function of SC. Lasers that ablate or disrupt SC are one available technique for facilitating drug permeation through skin. An ablative laser can remove SC in a precise and controlled manner (1). It irradiates skin without contact (2), and a very low fluence is needed to enhance drug permeation, ensuring the safety of this device (3). Full-surface ablative lasers are the modality most commonly used for laser-mediated drug delivery. Recently, fractional ablation, a new laser device, has been developed to maintain enhancement of drug penetration and achieve quicker SC recovery (4,5). It produces numerous microscopic treatment zones (MTZs) surrounded by unaffected tissues (6). Re-epithelialization can thus be accomplished within 12 to 24 h (2,7)—a significantly shorter period than conventional laser (3 to 4 days).

Skin permeation of topically applied drugs depends upon many factors, including release from vehicles, SC partitioning, drug clearance in skin, and the physicochemical characteristics of drugs. Among these, vehicle optimization is an important parameter governing drug penetration *via* skin. Most investigations of laser-assisted drug permeation focus on comparison of different permeants and laser conditions. Research comparing the effect of different vehicles as a variable has been lacking up to now. With this in mind, the present study aimed to elucidate the impact of different vehicles for laser-aided topical drug delivery systems.

Both conventional and fractional lasers were used in comparisons of vehicles. We used imiquimod as a model drug due to its moderate lipophilicity and great permeation enhancement by laser ablation (7). Topically applied imiquimod therapy is beneficial for treating warts, actinic keratosis, Bowen's disease and skin carcinomas (8). As is frequently reported, a 5% commercial imiquimod cream may lead to severe pain and skin irritation/erythema (9,10). Laser ablation may be an ideal method for enhancing imiquimod permeation, reducing the required dose and adverse effects. This study also used another drug for treating Bowen's disease and skin cancers (11) as a model permeant, 5-aminolevulinic acid (ALA), which has more hydrophilic properties compared to imiquimod (partition coefficient log $P = -1.5$ *versus* 2.7).

We prepared aqueous medium with water-soluble solvents as drug carriers: polyethylene glycol 400 (PEG 400), propylene glycol (PG), and ethanol. All are soluble in water. Lipid nanoparticles were also employed as carriers, because of their unique permeation manner compared to aqueous vehicles. This study mainly used *in vitro* Franz cells to examine drug delivery by laser irradiation of skin. An *in vivo* permeation experiment was performed by confocal laser scanning microscopy (CLSM) to determine ALA distribution in laser-treated skin.

MATERIALS AND METHODS

Materials

Imiquimod was purchased from LKT Laboratories (St. Paul, MN, USA). ALA, PEG 400, PG, ethanol and isopropyl myristate (IPM) were supplied by Sigma-Aldrich (St. Louis, MO, USA). Cellulose membrane (Cellu-Sep® T1, with a molecular weight cutoff of 3,500) was obtained from Membrane Filtration Products (Seguin, TX, USA). Strat-M® membrane for the skin diffusion test was a gift from Merck Millipore (Billerica, MA, USA).

Partition Coefficient (log P_{IPM}/vehicle) between Isopropyl Myristate (IPM) and Vehicle

A determined concentration of imiquimod in methanol was pipetted in test tubes. We used nitrogen gas to evaporate the methanol. IPM and vehicle (40% PEG 400, PG, or ethanol in water) with a volume of 1 ml were deposited in test tube. The tubes were stoppered and shaken for 6 h. Both IPM and aqueous phase were assayed by high performance liquid chromatography (HPLC) to quantify the amount of imiquimod. The HPLC analytical method was previously described (7).

Preparation of Donor Vehicles

Both supersaturated suspension and saturated solution of imiquimod were prepared in 40% PEG 400, PG, and ethanol in water. A dose of 0.08% (w/v) imiquimod was employed in supersaturated suspension. At this dose, imiquimod was not fully solubilized in the aqueous vehicles. The suspension was agitated for 24 h, and then centrifuged at 10,000 rpm for 10 min. The supernatant was collected as the saturated solution. The saturation concentration of imiquimod was determined by HPLC. A 0.64% dose was prepared for ALA vehicles. ALA could be completely solubilized in all vehicles tested.

Preparation of Lipid Nanoparticles

The lipid and water phases were prepared separately. The lipid phase was composed of 3% sesame oil, 3% cetyl palmitate, 0.3% Myverol, and imiquimod at a concentration of 0.08% in the final product. The water phase consisted of water with 4% Pluronic F68. Both phases were heated at 85°C for 15 min. The aqueous phase was then added into the lipid phase and mixed with a high-shear homogenizer (Pro250, Pro Scientific, Monroe, CT, USA) for 10 min. The mixture was further agitated by a probe-type sonicator (VCX600, Sonics and Materials, Newtown, CT, USA) for 10 min at 85°C. The nanosystems were employed in experiments after cooling to room temperature. The average particle size and zeta potential of the lipid nanoparticles were measured by photon correlation spectroscopy (Nano ZS90,

Malvern, Worcestershire, UK) after 100-fold dilution with water. The percentage of imiquimod encapsulated in nanoparticles was evaluated by ultracentrifugation (Optima MAX®, Beckman Coulter, Fullerton, CA, USA) (12).

Laser Assemblies

The full-surface ablative erbium:YAG laser (Contour, Sciton Laser, Palo Alto, CA, USA) is a device with a wavelength of 2,940 nm and a pulse duration of 100 μs. An ablation area of 1.5×1.5 cm^2 was created with a scanning handpiece. The laser irradiated skin after being calibrated to fluences of 2.5 and 5 J/cm^2, which produced ablative depths of 10 and 20 μm, respectively.

A fractional laser with pulse times of 60 and 80 μs for 2- and 4-mJ fluences was supplied by Lutronic (eCO_2®, San Jose, CA, USA). The microscopic columns of skin ablation were made with the handpiece. The diameter of MTZs was 120 μm. The scanning area of the handpiece was 1.2×1.2 cm^2. In 1 cm^2 there were 400 MTZ spots. The MTZ coverage in the scanned area was 7.3%.

Animals

Eight-week-old female nude mice (ICR-Foxn1nu) were purchased from the National Laboratory Animal Center (Taipei, Taiwan). The animal experiment followed guidelines set forth by the Guide for Laboratory Factlines and Care. The experimental protocol was approved by Institutional Animal Care and Use Committee of Chang Gung University.

In Vitro Transepidermal Water Loss (TEWL)

We used a Franz diffusion cell system to examine transepidermal water loss (TEWL) of nude mouse skin after exposure to donor vehicles *in vitro*. The dorsal region of nude mouse skin was mounted with the SC side facing towards the donor compartment. The receptor compartment was loaded with 20% ethanol in pH 7.4 buffer. The donor compartment was filled with 0.5 ml of 40% PEG 400, PG, or ethanol without drugs. The available diffusion area of the cell was 0.785 cm^2. The stirring rate and receptor temperature were maintained at 600 rpm and 37°C, respectively. After 24 h incubation with donor vehicles, we measured TEWL with a Tewameter® (TM300, Courage and Khazaka, Köln, Germany). The Tewameter® probe was positioned on the skin surface until a stable TEWL value ($g/m^2/h$) was attained. The laboratory temperature and relative humidity were kept at 26°C and 55%.

In Vitro Skin Permeation

The excised skin was pretreated by lasers before mounting in Franz cells. The SC-stripped skin was prepared if necessary (13). The setup of this experiment was the same as that used for TEWL examination. A 0.5-ml of imiquimod or ALA in various vehicles was the donor medium. At appropriate intervals, 300-μl aliquots in the receptor were withdrawn and replaced by an equal volume of fresh 20% ethanol/pH 7.4 buffer. The samples from the receptor were analyzed by HPLC.

Drug Amount in Hair Follicles

Differential stripping and cyanoacrylate skin surface biopsy were employed to quantify the amount of drug in follicles, as previously described (14). The skin was removed from Franz cell after application of vehicles for 24 h. SC was stripped with adhesive tapes 20 times. Subsequently a drop of superglue (ethyl cyanoacrylate 7004T, 3M, Taipei, Taiwan) was positioned on a glass slide, which was then pressed onto the surface of the stripped skin. The cyanoacrylate polymerized and the slide was removed by a quick movement after 5 min. The supernatant remaining on the slide was then scraped off, and placed in a test vial containing methanol (1 ml). The vial was shaken for 3 h. The methanol was then evaporated by vacuum. The mobile phase of HPLC was added to the vial for analysis.

In Vivo Skin Permeation with ALA

The dorsal region of nude mice was irradiated by lasers. Subsequently a glass cylinder with a diffusion area of 0.785 cm^2 was stuck on the dorsal skin with superglue. An ALA-containing vehicle (0.2 ml) was then pipetted into the cylinder. The administration period was 2 h, after which the mouse was sacrificed, and the treated skin excised and washed. We used CLSM (TCS SP2, Leica, Wetzlar, Germany) to scan the ALA distribution in the skin. The wavelengths of excitation and emission were set at 488 and 590 nm, respectively.

Statistical Analysis

All data were subjected to statistical analysis. The results are expressed as mean and standard deviation (S.D.). We used the unpaired Student's *t*-test to compare differences between formulations. The results were considered statistically significant at the level of $p < 0.05$.

RESULTS

In Vitro Skin Permeation with Imiquimod

In vitro imiquimod permeation was investigated with varying vehicles and fluences. We first evaluated supersaturated dispersion as a donor vehicle. The total amount of imiquimod that penetrated the skin was plotted against time, as shown in Fig. 1. The steady-state flux observed in Table I was

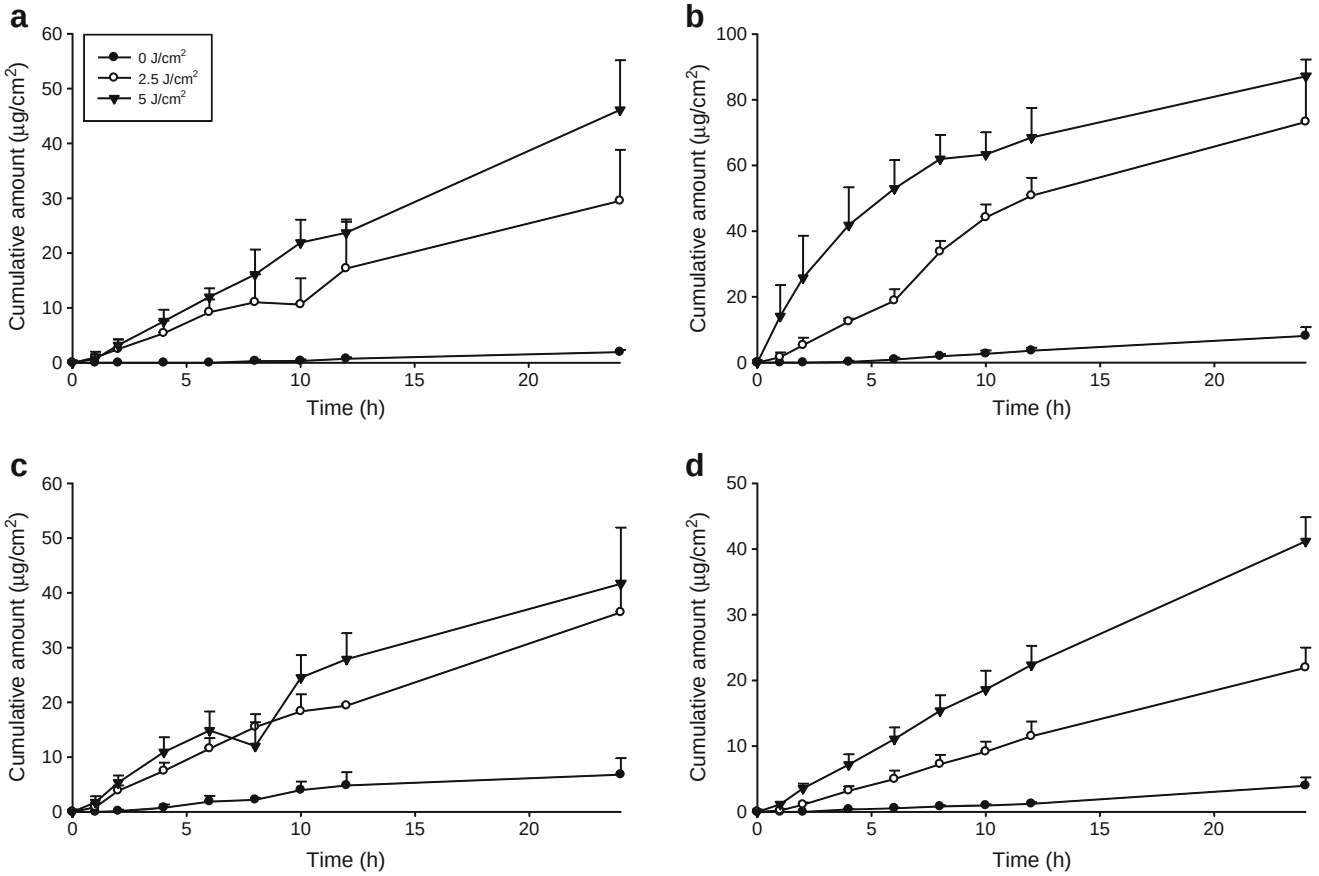

Fig. 1 *In vitro* cumulative amount-time profiles of imiquimod (0.08%, w/v) delivered by conventional laser treatment of nude mouse skin at 2.5 and 5 J/cm^2 using 40% PEG 400/water (**a**), PG/water (**b**), ethanol/water (**c**), and lipid nanoparticles (**d**) as vehicles. Each value represents the mean ± SD ($n = 4$).

computed from the slope of Fig. 1. Skin permeation with conventional laser treatment resulted in increased imiquimod flux. Irradiation at 2.5 J/cm^2 led to an increase of flux from 0.11 to 1.23 µg/cm^2/h using PEG 400 medium, giving an enhancement ratio (ER) of 12. An increase in fluence from 2.5 to 5 J/cm^2 resulted in further enhancement of penetration (ER = 18). The ER of PG and ethanol was significantly lower than that of PEG 400, with ethanol demonstrating the least enhancement by laser. Deeper ablation using higher fluence did not further increase imiqimod flux from the PG and ethanol vehicles. Lipid nanoparticles were also used as a carrier for imiquimod delivery, with nanocarriers exhibiting a size of 228.87 ± 1.64 nm, meeting the criteria for defining nanosized systems. The absolute zeta potential showed a value of −32.27 ± 0.47 mV. The percentage of imiquimod encapsulated in a lipid matrix of particles was 97.17 ± 0.56%, demonstrating a nearly complete loading in the lipid phase. When applying conventional laser at 2.5 and 5 J/cm^{2,} the mean flux of imiquimod was 5- and 10-fold greater than that of untreated controls, respectively.

Fractional ablation was less effective for enhancing imiquimod delivery compared to full-surface ablative laser. As with the conventional laser, PEG 400 generally showed the highest enhancement using the fractional laser, followed by PG and ethanol. The permeation profile of imiquimod using fractional laser treatment is shown in Fig. 2. The flux and ER with fractional laser are summarized in Table I. A 3- and 9-fold improvement of flux by 2 and 4 mJ compared to control group was observed. There was no increase ($p > 0.05$) in imiquimod flux by fractional laser when loading the drug in nanoparticulate form.

A further experiment using saturated solutions as donor vehicles was performed; this condition ensured a maximal and equal thermodynamic activity of imiquimod in all vehicles. Table II lists the flux, permeability coefficients (PC), and ER of imiquimod permeation from saturated vehicles. PC was measured from the flux divided by saturated concentration in the donor. Imiquimod concentrations in saturated solution were 298.82 ± 10.91, 548.04 ± 10.01, and 75.42 ± 1.44 µg/ml for 40% PEG 400, PG, and ethanol, respectively. The different vehicles clearly affected imiquimod delivery *via* skin. In the absence of laser exposure, the medium of 40% ethanol showed greater PC (12.91 cm/h × 10^{-3}) as compared to PEG 400 and PG ($p < 0.05$). Irradiation with full-surface ablative laser increased drug penetration from PEG 400 by a 26-fold.

Table I The *In Vitro* Flux ($\mu g/cm^2/h$) of Imiquimod (0.08%, w/v) *via* Nude Mouse Skin Treated With or Without Conventional and Fractional Lasers

Laser	Vehicle	Fluence	Flux ($\mu g/cm^2/h$)	ER
Conventional	40% PEG400	0 (control)	0.11 ± 0.01	–
		2.5 J/cm^2	1.23 ± 0.31	11.54
		5 J/cm^2	1.97 ± 0.34	18.45
	40% PG	0 (control)	0.38 ± 0.11	–
		2.5 J/cm^2	3.27 ± 0.65	8.52
		5 J/cm^2	2.93 ± 0.33	7.62
	40% ethanol	0 (control)	0.32 ± 0.14	–
		2.5 J/cm^2	1.51 ± 0.19	4.75
		5 J/cm^2	1.73 ± 0.39	5.45
	nanoparticles	0 (control)	0.18 ± 0.06	–
		2.5 J/cm^2	0.95 ± 0.13	5.36
		5 J/cm^2	1.74 ± 0.14	9.76
Fractional	40% PEG400	2 mJ	0.28 ± 0.03	2.61
		4 mJ	0.94 ± 0.11	8.83
	40% PG	2 mJ	0.50 ± 0.05	1.31
		4 mJ	1.58 ± 0.06	4.12
	40% ethanol	2 mJ	0.67 ± 0.04	2.12
		4 mJ	0.88 ± 0.09	2.76
	nanoparticles	2 mJ	0.25 ± 0.05	1.43
		4 mJ	0.23 ± 0.07	1.29

ER enhancement ratio of the flux of laser-treated group/the flux of untreated control group

Each value represents the mean and S.D. ($n = 4$)

This enhancement was significantly higher than that observed with PG and ethanol vehicles. A similar trend was observed when using fractional laser, though the level of enhancement was less than that of conventional laser.

In Vitro Skin Permeation *via* Various Barriers

To explore mechanisms of drug delivery *via* laser-treated skin, different types of penetration barriers were employed for *in vitro* delivery. In this experiment, the 40% PEG 400/water and nanoparticles were selected as carriers for imiquimod (Fig. 3a and b). SC was removed to investigate its role in imiquimod permeation. The stripping significantly increased ($p<0.05$) imiquimod flux from PEG 400 by a 9-fold. Flux from nanoparticles *via* stripped skin was six times greater than that *via* untreated skin. We showed that conventional laser was superior to SC stripping ($p<0.05$) for enhancing drug permeation.

A possible rate-limiting step in skin delivery is the release from formulations. We used a cellulose membrane without barrier function to examine release behavior. It showed a thickness of 28 μm, which was derived from cotton cellulose by glycerin treatment. As depicted in Fig. 3a, the amount of imiquimod release from PEG 400 exceeds penetration across stripped skin. This demonstrates that viable skin plays some role in blocking permeation with imiquimod. This phenomenon was not observed for nanosystems, since the flux across stripped skin and cellulose membrane was comparable ($p>0.05$). Instead of using animal skin, we employed Strat-M® to detect the amount of imiquimod in the receptor. This membrane is an alternative for skin diffusion testing developed by Merck Millipore. The thickness of this membrane is 300 μm. The predominant materials of Strat-M® are polyethersulfone and polyolefin post-treated by lipids. As depicted in Fig. 3a, there was higher permeation of imiquimod across Strat-M® compared with intact nude mouse skin ($p<0.05$). When we incorporated the drug in nanoparticles, we observed similar flux between Strat-M® and nude mouse skin ($p>0.05$) as shown in Fig. 3b, demonstrating that Strat-M® is a good substitute for animal skin in this case.

Drug Amount in Hair Follicles

The appendageal route may be a significant pathway for drug delivery *via* skin. Using this approach, the amount of imiquimod accumulated in follicles was determined. Using the PEG 400 vehicle, 0.80±0.22 μg/cm^2 of the drug was recovered from follicles of intact skin. Drug deposition in follicles was found to rise 7-fold upon conventional laser treatment, as shown in Fig. 4. Nevertheless, use of fractional laser did not promote imiquimod deposition ($p>0.05$). Neither type of laser could enhance follicular drug accumulation from lipid nanoparticles ($p>0.05$).

In Vivo Skin Permeation with ALA

ALA is a hydrophilic molecule. We evaluated laser-aided ALA delivery for comparison with lipophilic imiquimod. Figure 5a and b show cumulative amount-time profiles of ALA with exposure to full-surface ablative laser and fractional laser. Both lasers increased ALA permeation. As shown in Table III, flux of pH 5 buffer by conventional laser was 641 times greater than that of the control group. The ER for 40% PEG and PG was 445 and 104, respectively. Full-surface ablation facilitated diffusion of ALA in a more efficient way than imiquimod. ALA flux *via* fractional laser-treated skin was 41- and 5-fold greater as compared to passive permeation, respectively, when pH 5 buffer and 40% PEG400 were employed as carriers. ALA permeation with 40% PG was not increased by fractional laser ($p>0.05$).

In Vivo Skin Permeation of ALA

ALA in pH 5 buffer and 40% PG were administered to dorsal skin of nude mice and biopsies were analyzed by CLSM after application for 2 h. ALA is bioconverted into proporphyllin

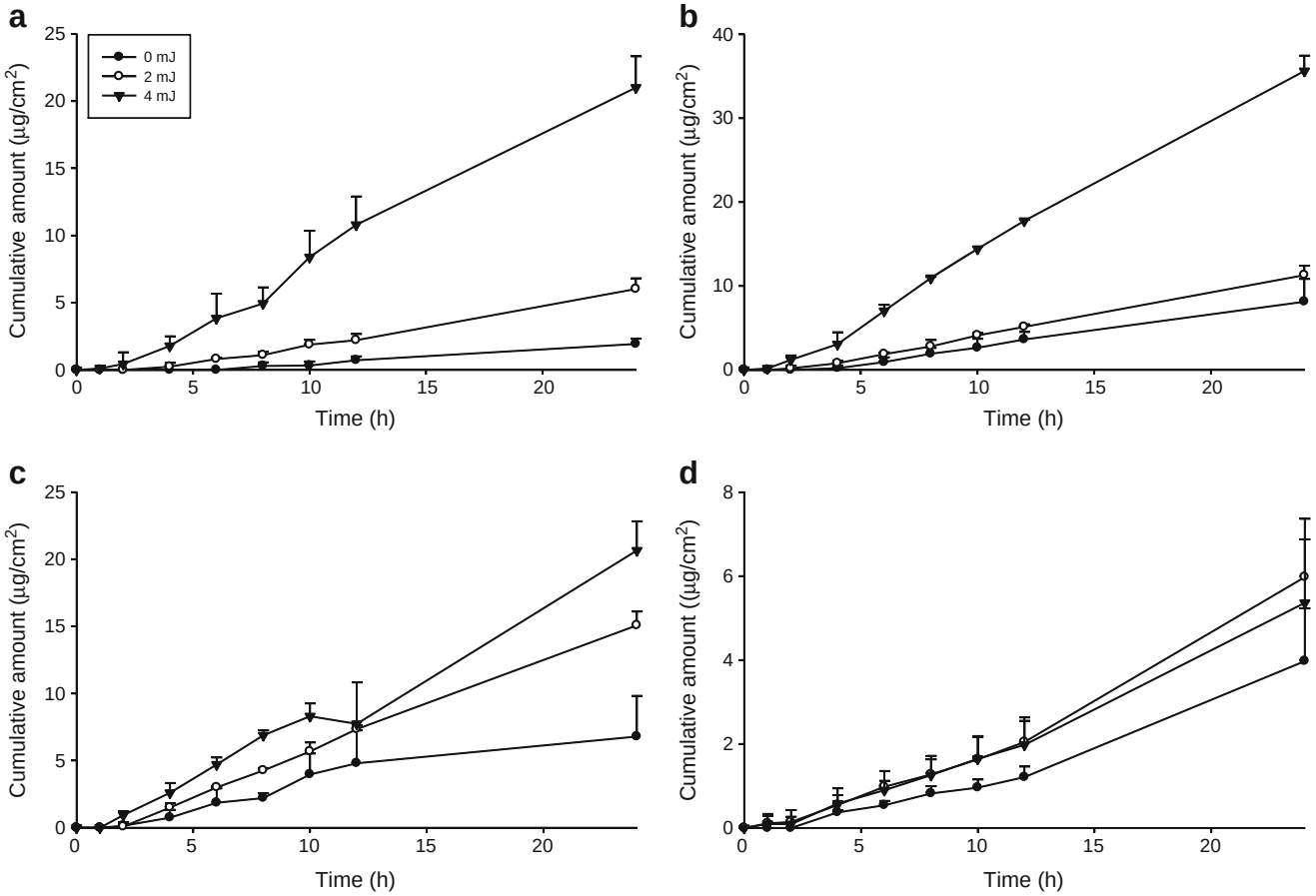

Fig. 2 *In vitro* cumulative amount-time profiles of imiquimod (0.08%, w/v) delivered by fractional laser treatment of nude mouse skin at 2 and 4 mJ using 40% PEG 400/water (**a**), PG/water (**b**), ethanol/water (**c**), and lipid nanoparticles (**d**) as vehicles. Each value represents the mean ± SD ($n = 4$).

IX (PpIX) after entering into cytoplasm. The expression of PpIX in cells exhibited red fluorescence. As shown in Fig. 6a, no autofluorescence was observed from intact skin that received no treatment. A faint red signal was detected in the intact skin after treatment with ALA-containing buffer and PG vehicles (Fig. 6b and c). As expected, fluorescence was

Table II The *In Vitro* Flux ($\mu g/cm^2/h$) of Imiquimod from Vehicles with Saturated Solubility *via* Nude Mouse Skin Treated With or Without Conventional and Fractional Lasers

Laser	Vehicle	Fluence	Flux ($\mu g/cm^2/h$)	PC ($cm/h \times 10^{-3}$)	ER
Conventional	40% PEG400	0 (control)	0.11 ± 0.03	0.37 ± 0.08	–
		2.5 J/cm²	1.61 ± 0.13	5.51 ± 0.70	14.89
	40% PG	0 (control)	0.35 ± 0.06	0.65 ± 0.16	–
		2.5 J/cm²	0.99 ± 0.07	1.81 ± 0.12	2.78
	40% ethanol	0 (control)	0.97 ± 0.28	12.91 ± 3.71	–
		2.5 J/cm²	1.34 ± 0.11	17.78 ± 1.48	1.38
Fractional	40% PEG400	4 mJ	0.64 ± 0.11	2.13 ± 0.37	5.76
	40% PG	4 mJ	0.31 ± 0.07	0.58 ± 0.13	0.89
	40% ethanol	4 mJ	1.53 ± 0.24	20.31 ± 3.18	1.57

PC permeability coefficient = flux/saturated solubility

ER enhancement ratio of the flux of laser-treated group/the flux of untreated control group

Each value represents the mean and S.D. ($n = 4$)

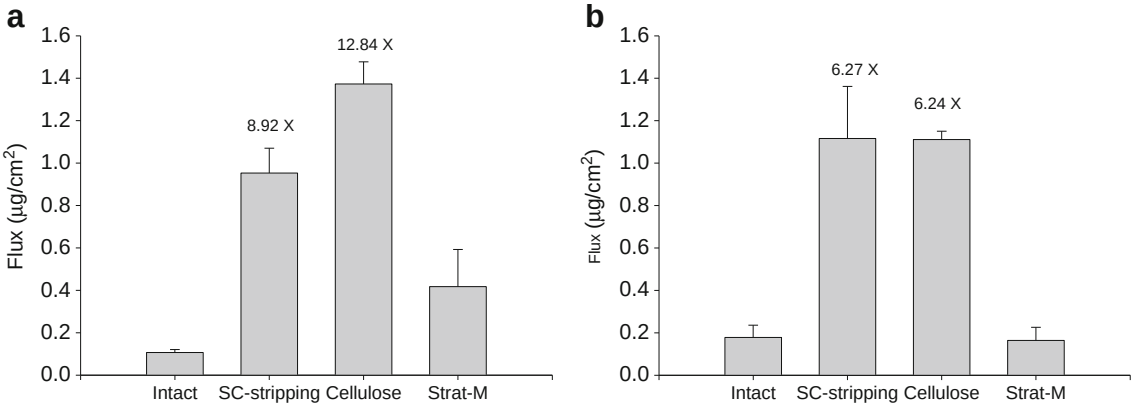

Fig. 3 *In vitro* imiquimod flux *via* intact skin, SC-stripped skin, cellulose membrane, and Strat-M® membrane using 40% PEG 400/water (**a**) and lipid nanoparticles (**b**) as vehicles. Each value represents the mean ± SD ($n = 4$).

visually apparent in the skin treated by conventional laser (Fig. 6d and e). Aqueous buffer provided stronger PpIX signaling than PG did. Skin irradiated with the fractional laser showed weaker fluorescence intensity compared with the full-surface ablative modality (Fig. 6f and g).

DISCUSSION

Although various drugs or macromolecules have been linked with the benefits of laser-assisted permeation, no study has been conducted to explore the influence of drug vehicles. There are thus no standard recommendations for feasible vehicle formulations for laser-mediated delivery. Our results suggest enhanced skin delivery of imiquimod by both conventional and fractional laser modalities. The ER ranged between 1 and 19, depending upon drug carriers selected. It is desirable to reduce the applied dose of imiquimod, since this drug elicits erythema in most patients (15). The predominant reason that lasers enhance permeation is that ablation of SC reduces drug delivery barriers. According to previous studies, some remnants of SC were present at the lower fluence using both conventional (2.5 J/cm^2) and fractional (2 mJ) lasers (12,16). The photomechanical wave generated by lasers is another mechanism for eliciting lacunar space expansion, thus creating micropores in remnant SC (17,18). Higher fluence with conventional (5 J/cm^2) and fractional (4 mJ) laser modalities could not only ablate the whole SC but also the superficial epidermis. Our results indicated that the imiquimod permeation through higher fluence-treated skin was significantly greater than through SC-stripped skin. This demonstrates that SC is not the sole barrier to imiquimod delivery. The barrier function of varying layers of epidermis could not be ignored in this case.

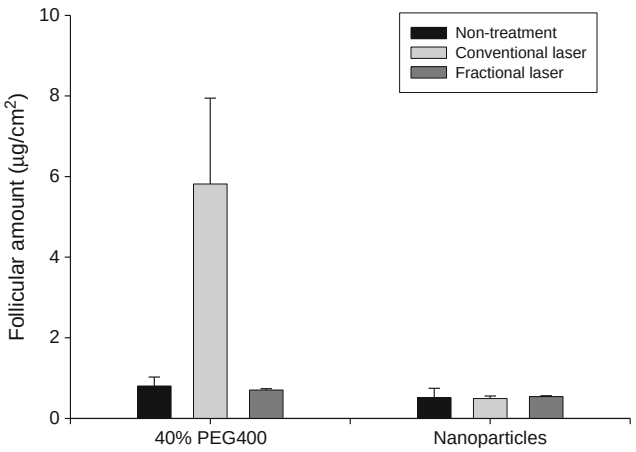

Fig. 4 The imiquimod amount in hair follicles (μg/cm^2) of nude mouse skin after topical application with or without conventional and fractional lasers. Each value represents the mean ± SD ($n = 4$).

Fractional resurfacing is a new fashion in laser treatment which has been promoted as a safer modality that allows a more rapid healing rate (19). However, fractional laser was less effective for enhancing delivery of both imiquimod and ALA than full-surface ablative laser. This could be because only a partial ablation of the total diffusion area was irradiated with fractional laser. MTZs occupied 7.3% of the scanned area. However, the difference in permeation enhancement between both the two lasers was smaller than the difference in ablative areas. This indicates a more-efficient enhancement by fractional laser. Fractional irradiation produced cylinder-shaped microchannels in the skin. In addition to vertical diffusion of permeant into deeper strata, the permeant can diffuse into surrounding skin tissues by a lateral route, as illustrated in Fig. 7. The increase in diffusion area with MTZ formation can lead to more efficient delivery of the drugs (20).

During the process of drug permeation *via* skin, drug molecules must be first released from the vehicle formulation. Subsequently the drug partitions from the vehicle pass into the SC layers. After sufficient accumulation in the SC, the permeant then diffuses into deeper strata by concentration

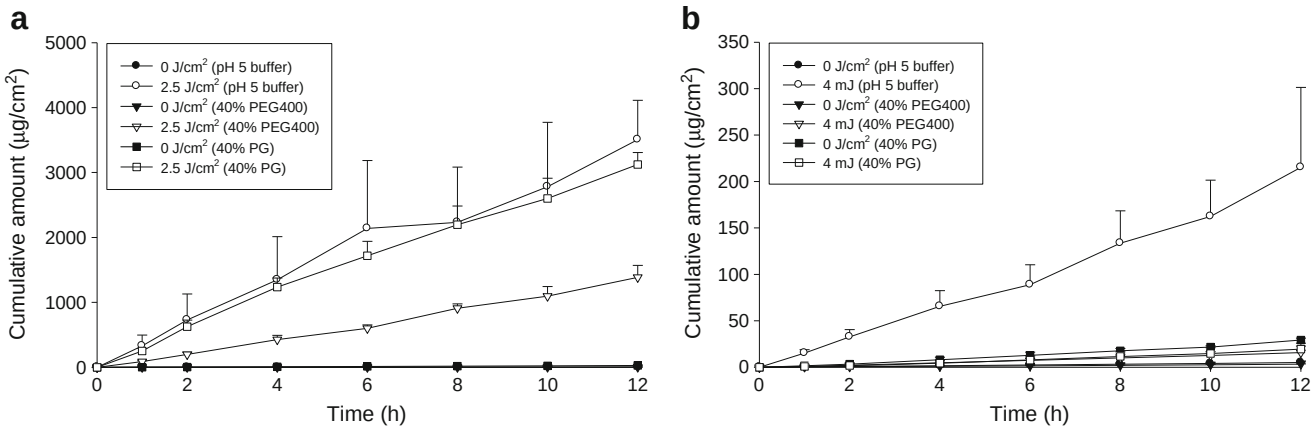

Fig. 5 *In vitro* cumulative amount-time profiles of ALA (0.64%, w/v) by conventional laser treatment (**a**) and fractional laser treatment (**b**) of nude mouse skin from pH 5 buffer, 40% PEG 400/pH 5 buffer, and PG/pH 5 buffer. Each value represents the mean ± SD ($n = 4$).

gradient (Fig. 7). Skin disruption by vehicles may have a substantial influence on the outcome of drug penetration. In order to understand whether the tested vehicles compromised skin integrity, *in vitro* TEWL was examined after a 24-h incubation. TEWL is an indicator for evaluating macroscopic alteration of SC barrier characterization. The values of TEWL obtained by application of PEG 400, PG, ethanol, and nanoparticles were 12.3±3.7, 10.9±4.1, 12.7±2.1, and 9.8±3.0 g/m^2/h, all approximating the values for untreated controls (11.1±2.5 g/m^2/h, $p > 0.05$). This may indicate the skin structure remains intact after vehicle application. Skin disruption and enhancement of drug permeation by the influence of vehicles can thus be ruled out.

The experimental results of imiquimod flux (supersaturated dispersion) and PC (saturated solution) revealed the general pattern of ethanol > PG > PEG400. The influence of cosolvents on skin drug delivery is primarily attributable to drug solubility and the partitioning ability of SC. PEG 400 is the cosolvent with the highest polarity (log $P = -4.8$), followed by PG (−0.9) and ethanol (2.6). Imiquimod solubility increased in the order of PG > PEG 400 > ethanol. Although imiquimod is basically recognized a lipophilic drug (21), its solubility in 40% ethanol was very low. This may be due to poor solvation of imiquimod with ethanol, although ethanol exhibited a less polarity as one of its properties. The low solubility of imiquimod in ethanol is supported by previous reports (22,23). The molecules should be in the solubilized form for penetrating skin. However, our results demonstrated that higher drug solubility in vehicles did not produce greater permeation *via* intact skin. The results of PC suggest that solubility has a negligible influence on imiquimod permeation. The precipitation of imiquimod in the supersaturated formulation can partly explain the fact that PEG 400 had the lowest permeation (without lasers) of all the vehicles. Donnelly *et al.* (24) suggest that imiquimod precipitation due to excessive concentration over solubility prevents its release. The large amount of imiquimod precipitate in the PEG 400 supersaturated dispersion led to lower flux as compared to PG. Nevertheless, this mechanism cannot explain the fact that the highest permeation (without lasers) was attained from 40% ethanol, although this cosolvent had a very low solubility. A possible explanation is the dislike of imiquimod for 40% ethanol due to poor solvation. Imiquimod prefers partitioning into SC to escape from this vehicle.

Table III The *In Vitro* Flux (μg/cm^2/h) of ALA (38 mM) *via* Nude Mouse Skin Treated With or Without Conventional and Fractional Lasers

Laser	Vehicle	Fluence	Flux (μg/cm^2/h)	ER
Conventional	pH 5 buffer	0 (control)	0.43±0.14	–
		2.5 J/cm^2	272.78±52.36	641.27
	40% PEG400	0 (control)	0.26±0.03	–
		2.5 J/cm^2	116.66±13.99	444.75
	40% PG	0 (control)	2.45±0.07	–
		2.5 J/cm^2	254.1318.80	103.67
Fractional	pH 5 buffer	4 mJ	17.54±6.04	41.23
	40% PEG400	4 mJ	1.75±0.34	5.14
	40% PG	4 mJ	1.69±0.24	0.69

ER enhancement ratio of the flux of laser-treated group/the flux of untreated control group

Each value represents the mean and S.D. ($n = 4$)

The cosolvents appeared to change imiquimod solubility in SC. SC uptake of more lipophilic vehicles improved the solubility of lipophilic drugs in SC (25). SC is naturally lipophilic and far more accessible to non-polar than polar vehicles. PG and ethanol were the cosolvents with less polarity, and exhibited higher imiquimod penetration than PEG 400 in the absence of lasers. Both PG and ethanol have been proven to be easily partitioned into SC, increasing drug solubility in SC (26,27). Previous researches (27,28) also indicates that ethanol/water systems have superior interaction with SC compared to PG/water systems. An abundant partitioning of ethanol into SC promoted diffusion of imiquimod into skin.

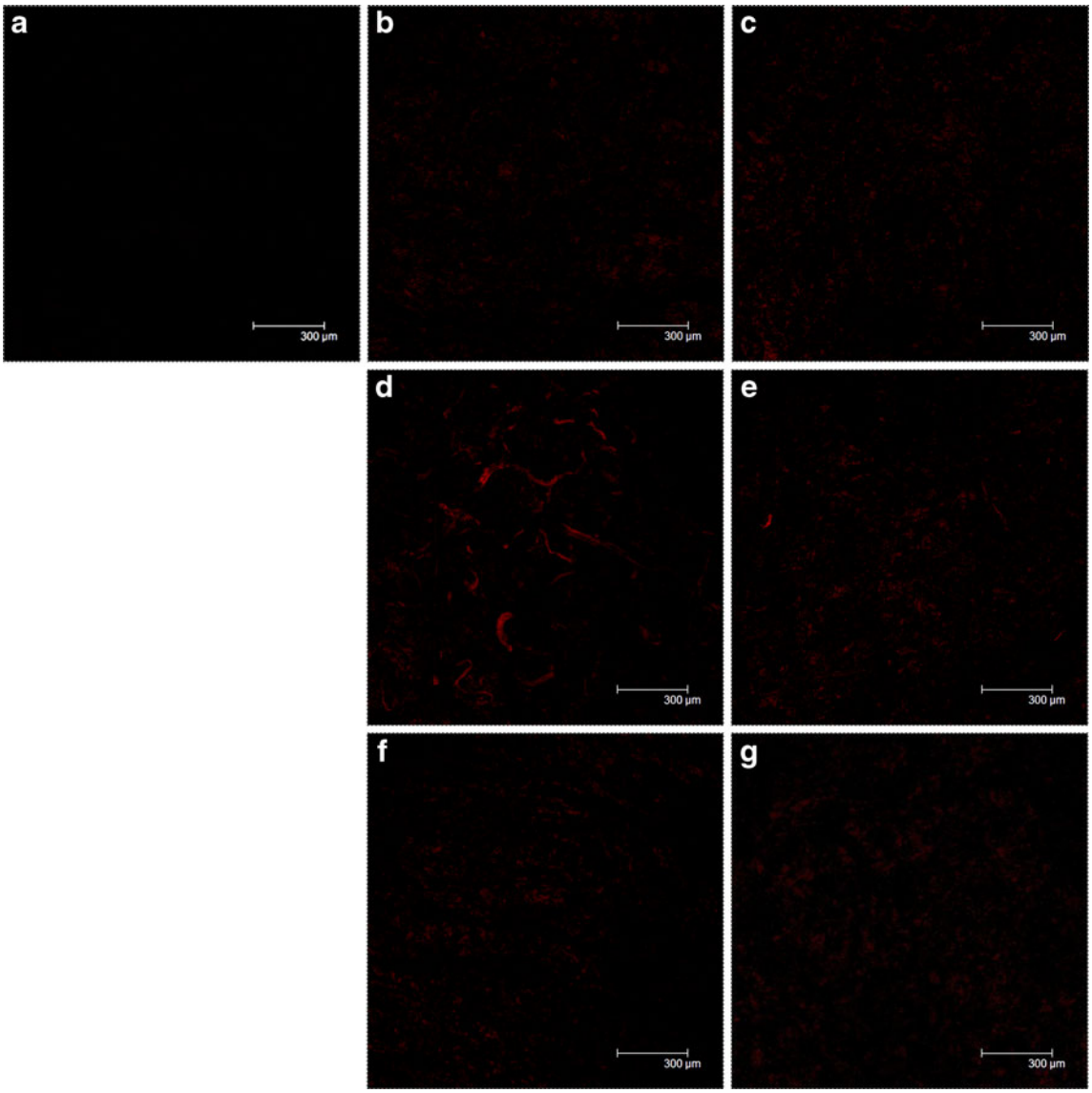

Fig. 6 Confocal micrographs of nude mouse skin: blank skin without any treatment (**a**); *in vivo* application of ALA in pH 5 buffer *via* untreated skin for 2 h (**b**); *in vivo* application of ALA in 40% PG/pH 5 buffer *via* untreated skin for 2 h (**c**); *in vivo* application of ALA in pH 5 buffer *via* conventional laser-treated skin for 2 h (**d**); *in vivo* application of ALA in 40% PG/pH 5 buffer *via* conventional laser-treated skin for 2 h (**e**); *in vivo* application of ALA in pH 5 buffer *via* fractional laser-treated skin for 2 h (**f**); *in vivo* application of ALA in 40% PG/pH 5 buffer *via* fractional laser-treated skin for 2 h (**g**). Skin thickness was optically scanned at 5-μm increments through the Z-axis for a total 70-μm depth. The image is a summary of 15 fragments at various skin depths.

IPM is an organic medium regarded as simulating SC lipids (29). We determined the log $P_{\mathrm{IPM/vehicle}}$ of different cosolvents. As expected, 40% ethanol demonstrated the highest log $P_{\mathrm{IPM/vehicle}}$ for imiquimod (-0.66 ± 0.03), followed by PG (-0.73 ± 0.05) and PEG 400 (-1.92 ± 0.29). These results confirmed the easier partitioning of ethanol into SC.

In laser-assisted imiquimod delivery, permeation enhancement by various vehicles showed an opposite trend when compared with diffusion across untreated skin: imiquimod in PEG 400 demonstrated the greatest enhancement, followed by PG and ethanol. After laser ablation, the resistance from SC was diminished and an aqueous pathway for the drugs was created. The permeation profiles of SC-stripped skin suggested viable skin plays a partial role in imiquimod diffusion. Laser treatment led to direct contact of vehicles with the epidermis, especially with higher fluence. Permeants should diffuse out of vehicles to partition into the hydrophilic epidermis.

Unlike penetration of intact skin, laser exposure facilitated miscibility of polar cosolvents into epidermis. This fusion of polar cosolvents and epidermis formed a drug reservoir with improved drug partitioning (Fig. 7). Haak *et al.* (5) also demonstrated easier penetration of PEG 400 molecules into laser-treated skin. Some differences can be found in cosolvent

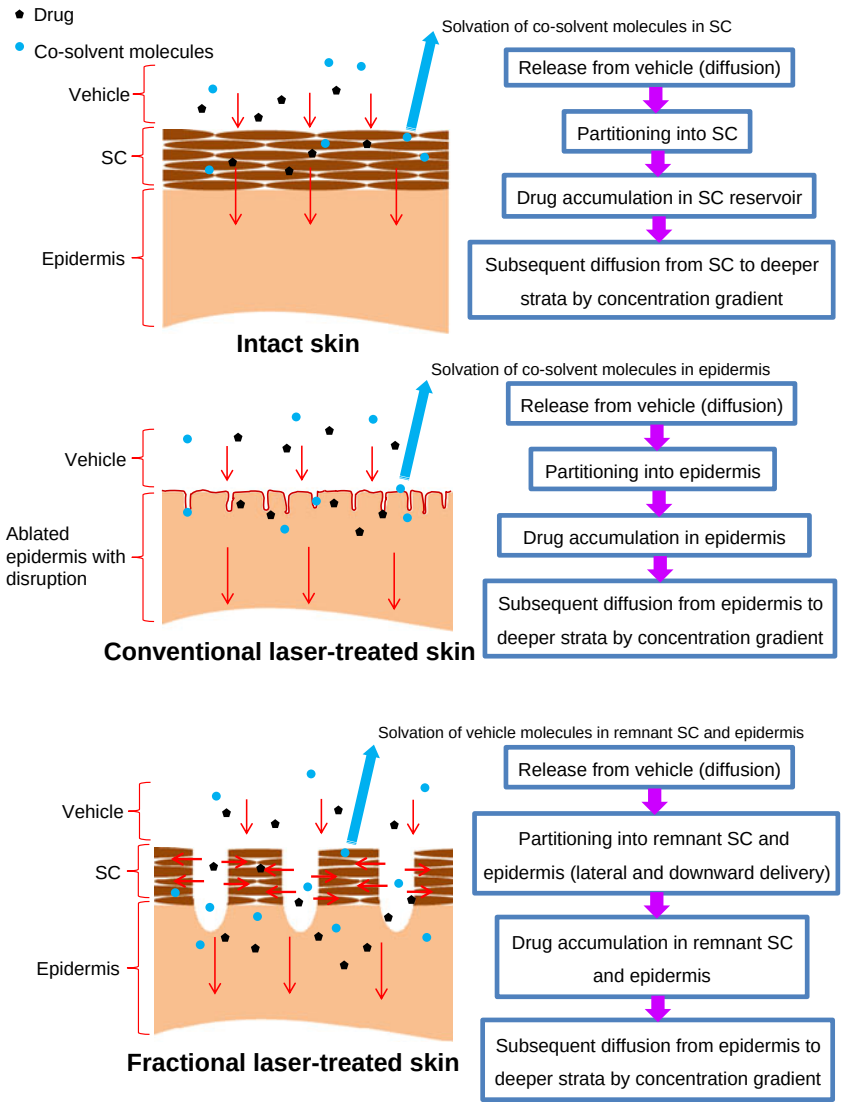

Fig. 7 A scheme showing the possible process and mechanism of drug delivery *via* intact, conventional laser-treated, and fractional laser-treated skin.

diffusion using conventional and fractional lasers. Because of the reservation of some intact SC above the epidermis, cosolvents can partition into either SC or epidermis (Fig. 7). This explains the smaller discrepancy in imiquimod delivery enhancement among vehicles when using fractional laser (ER ranged from 1.55 to 3.27) rather than conventional laser (ER ranged from 1.38 to 14.89).

Lasers moderately enhanced imiquimod delivery from nanoparticles. The enhancement generally did not surpass the level achieved with aqueous vehicles. The nanoparticulate permeation process was somewhat different from the cosolvent-containing medium. There were two pathways for drug delivery from nanoparticles. One pathway consisted of the drug's release from the lipid matrix to the aqueous phase, and then from the external phase to SC (30). Another pathway was the fusion of lipid nanoparticles with SC, followed by direct drug release from the nanoparticles into SC. Imiquimod release from nanoparticles across cellulose membranes reflected slow release from the lipid matrix. Lipid exchange can occur between lipid nanoparticles and SC lipids after nanoparticulate fusion into SC (31). SC removal with lasers significantly eliminated this effect, resulting in less enhancement of drug penetration compared with free imiquimod in PEG 400. SC stripping obtained only a 6-fold increase of imiquimod flux. This may reveal an essential reservoir of lipophilic SC for nanoparticulate partitioning into skin. Although the nanoparticulate fusion to SC was retarded by laser ablation, moderate permeation enhancement was still achieved using nanoparticles as a carrier. SC was not the only layer of importance with respect to nanoparticulate delivery. Epidermis also played some role. The ablative laser not only removed SC, it may also permeabilize epidermis by irradiation with photomechanical waves or laser-mediated thermal effect (Fig. 7).

Hair follicles are likely to play an important role in skin drug delivery, as hair follicles are an efficient route to deliver drugs into deeper skin strata. Permeants with log *P* of >2 demonstrated minimal entrance into follicles (32). Imiquimod possesses a log *P* of 2.7 and has revealed a potent selectivity for follicles after full-surface ablative laser exposure. Our previous study (33) suggested that laser can propagate ablation effect around follicles. Inactive follicles can be opened by ablation for effective drug diffusion. On the other hand, fractional laser did not raise imiquimod accumulation in follicles. Since the area of follicles only occupies a limited space of skin surface, it is difficult to precisely irradiate only follicles with MTZs. Though some types of nanoparticles tend to accumulate in follicles (12,34), this was not evident in the present study; the lasers did not change follicular delivery of imiquimod in lipid nanoparticles.

Our results showed that lasers achieved greater enhancement of ALA (hydrophilic permeant) permeation compared to imiquimod (lipophilic permeant). Lasers are thus helpful for ALA therapy, since this drug has poor penetration through keratinized skin above skin tumors (35). Since ALA is totally soluble in aqueous buffer without a cosolvent, we employed a pH 5 buffer as the ALA vehicle. Maximum penetration enhancement by lasers was observed with the pH 5 buffer according to *in vitro* and *in vivo* experiments. This result was consistent with the finding that the polar vehicles provided higher enhancement of drug delivery for imiquimod. PG exhibited the least ALA permeation enhancement. Araújo *et al.* (36) demonstrated easy diffusion of ALA from PG-containing vehicles. SC removal significantly reduced the effect of PG diffusion, resulting in more limited enhancement using laser-assisted ALA delivery. It is acknowledged that it is hard to partition and diffuse a hydrophilic permeant into lipophilic SC. Even though this may be true, based on the experimental data, ALA permeation from various vehicles followed the same trend as imiquimod permeation, demonstrating that the same rule governs ALA and imiquimod delivery *via* intact and laser-treated skins. Previous studies (37,38) have shown that SC remains an important reservoir for ALA partitioning.

CONCLUSIONS

In summary, the ablative lasers were more effective for promoting drug molecules into skin. They may be considered a potential technique for increasing skin delivery of both lipophilic and hydrophilic drugs. This enhanced delivery is vital for both drugs, so as to reduce the required dose and avoid skin irritation. The conventional laser provided better performance for promoting drug permeation than the fractional laser. However, the fractional laser was an efficient mode for increasing drug delivery through skin after consideration of the ablative percentage on the skin surface. Different drug delivery vehicles had an important effect on laser-assisted permeation. Diffusion of cosolvent molecules into skin and partitioning of the drugs between skin and vehicle are the factors governing effectiveness of vehicles for drug delivery through skin. The formulations with polar characteristics, such as aqueous buffer and PEG 400, exhibited better laser-assisted drug delivery enhancement compared to less-polar vehicles. Laser-mediated delivery with nanoparticles did not surpass that of polar vehicles, because of the difficulty of fusing lipid matrix with ablated skin. We conclude that choosing the optimal vehicle for laser-supported drug delivery substantially affects permeation and is therefore important for successful outcomes.

REFERENCES

1. Lee WR, Shen SC, Fang CL, Zhuo RZ, Fang JY. Topical delivery of methotrexate via skin pretreated with physical enhancement techniques: low-fluence erbium:YAG laser and electroporation. Lasers Surg Med. 2008;40:468–76.
2. Lee WR, Shen SC, Al-Suwayeh SA, Yang HH, Li YC, Fang JY. Skin permeation of small-molecule drugs, macromolecules, and nanoparticles mediated by a fractional carbon dioxide laser: the role of hair follicles. Pharm Res. 2013;30:792–802.
3. Chen X, Shah D, Kositratna G, Manstein D, Anderson RR, Hædersdal M. Facilitation of transcutaneous drug delivery and vaccine immunization by a safe laser technology. J Control Release. 2012;159:43–51.
4. Lee WR, Shen SC, Pai MH, Yang HH, Yuan CY, Fang JY. Fractional laser as a tool to enhance the skin permeation of 5-aminolevulinic acid with minimal skin disruption: a comparison with conventional erbium:YAG laser. J Control Release. 2010;145:124–33.
5. Haak CS, Bhayana B, Farinelli WA, Anderson RR, Hædersdal M. The impact of treatment density and molecular weight for fractional laser-assisted drug delivery. J Control Release. 2012;163:335–41.
6. Ong MWS, Bashir SJ. Fractional laser resurfacing for acne scars: a review. Br J Dermatol. 2012;166:1160–9.
7. Lee WR, Shen SC, Al-Suwayeh SA, Yang HH, Yuan CY, Fang JY. Laser-assisted topical drug delivery by using a low-fluence fractional laser: imiquimod and macromolecules. J Control Release. 2011;153:240–8.
8. Metcalf S, Crowson AN, Naylor M, Haque R, Cornelison R. Imiquimod as an antiaging agent. J Am Acad Dermatol. 2007;56:422–5.
9. Salasche S, Shumack S. A review of imiquimod 5% cream for the treatment of various dermatological conditions. Clin Exp Dermatol. 2003;28:1–3.
10. Hadley G, Derry S, Moore RA. Imiquimod for actinic keratosis: systematic review and meta-analysis. J Invest Dermatol. 2006;126:1251–5.
11. Musiol R, Serda M, Polanski J. Prodrugs in photodynamic anticancer therapy. Curr Pharm Des. 2011;17:3548–59.
12. Lin YK, Al-Suwayeh SA, Leu YL, Shen FM, Fang JY. Squalene-containing nanostructured lipid carriers promote percutaneous absorption and hair follicle targeting of diphencyprone for treating alopecia areata. Pharm Res. 2013;30:435–46.

13. Lanke SSS, Kolli CS, Strom JG, Banga AK. Enhanced transdermal delivery of low molecular weight heparin by barrier perturbation. Int J Pharm. 2009;365:26–33.
14. Teichmann A, Jacobi U, Ossadnik M, Richter H, Koch S, Sterry W, *et al.* Differential stripping: determination of the amount of topically applied substances penetrated into the hair follicles. J Invest Dermatol. 2005;125:264–9.
15. Swanson N, Abramovits W, Berman B, Kulp J, Rigel DS, Levy S. Imiquimod 2.5% and 3.75% for the treatment of actinic keratoses: results of two placebo-controlled studies of daily application to the face and balding scalp for two 2-week cycles. J Am Acad Dermatol. 2010;62:582–90.
16. Lee WR, Shen SC, Al-Suwayeh SA, Li YC, Fang JY. Erbium:YAG laser resurfacing increases skin permeability and the risk of excessive absorption of antibiotics and sunscreens: the influence of skin recovery on drug absorption. Toxicol Lett. 2012;211:150–8.
17. Menon GK, Kollias N, Doukas AG. Ultrastructural evidence of stratum corneum permeabilization induced by photomechanical waves. J Invest Dermatol. 2003;121:104–9.
18. Liu C, Zhang J, Yue Y, Luo Q, Zhu D. 1064 nm-Nd:YAG lasers with different output modes enhancing transdermal delivery: physical and physiological mechanisms. J Biomed Opt. 2013;18:061228.
19. El-Domyati M, Abd-El-Raheem T, Abdel-Wahab H, Medhat W, Hosam W, El-Fakahany H, *et al.* Fractional versus ablative erbium-yttrium-aluminum-garnet laser resurfacing for facial rejuvenation: an objective evaluation. J Am Acad Dermatol. 2013;68:103–12.
20. Bachhav YG, Heinrich A, Kalia YN. Using laser microporation to improve transdermal delivery of diclofenac: increasing bioavailability and the range of therapeutic applications. Eur J Pharm Biopharm. 2011;78:408–14.
21. Schön MP, Schön M. Imiquimod: mode of action. Br J Dermatol. 2007;157 Suppl 2:8–13.
22. Chollet JL, Jozwiakowski MJ, Phares KR, Reiter MJ, Roddy PJ, Schultz HJ, *et al.* Development of a topically active imiquimod formulation. Pharm Develop Technol. 1999;4:35–43.
23. Ramineni SK, Cunningham LL, Dziubla TD, Puleo DA. Development of imiquimod-loaded mucoadhesive films for oral dysplasia. J Pharm Sci. 2013;102:593–603.
24. Donnelly RF, McCarron PA, Zawislak AA, Woolfson AD. Design and physicochemical characterization of a bioadhesive patch for dose-controlled topical delivery of imiquimod. Int J Pharm. 2006;307:318–25.
25. Watkinson RM, Guy RH, Oliveira G, Hadgraft J, Lane ME. Optimisation of cosolvent concentration for topical drug delivery III–Influence of lipophilic vehicles on ibuprofen permeation. Skin Pharmacol Physiol. 2011;24:22–6.
26. Herkenne C, Naik A, Kalia YN, Hadgraft J, Guy RH. Effect of propylene glycol on ibuprofen absorption into human skin in vivo. J Pharm Sci. 2008;97:185–97.
27. Panchagnula R, Salve PS, Thomas NS, Jain AK, Ramarao P. Transdermal delivery of naloxone: effect of water, propylene glycol, ethanol and their binary combinations on permeation through rat skin. Int J Pharm. 2001;219:95–105.
28. Watkinson RM, Guy RH, Hadgraft J, Lane ME. Optimisation of cosolvent concentration for topical drug delivery–II: influence of propylene glycol on ibuprofen permeation. Skin Pharmacol Physiol. 2009;22:225–30.
29. Garzon LC, Martinez F. Temperature dependence of solubility for ibuprofen in some organic and aqueous solvents. J Sol Chem. 2004;33:1379–95.
30. Fang JY, Fang CL, Liu CH, Su YH. Lipid nanoparticles as vehicles for topical psoralen delivery: solid lipid nanoparticles (SLN) versus nanostructured lipid carriers (NLC). Eur J Pharm Biopharm. 2008;70:633–40.
31. Schäfer-Korting M, Mehnert W, Korting HC. Lipid nanoparticles for improved topical application of drugs for skin diseases. Adv Drug Deliv Rev. 2007;59:427–43.
32. Frum Y, Bonner MC, Eccleston GM, Meidan VM. The influence of drug partition coefficient on follicular penetration: in vitro human skin studies. Eur J Pharm Sci. 2007;30:280–7.
33. Lee WR, Shen SC, Liu CJ, Fang CL, Hu CH, Fang JY. Erbium: YAG laser-mediated oligonucleotide and DNA delivery via the skin: an animal study. J Control Release. 2006;115:344–53.
34. Zhang LW, Monteiro-Riviere NA. Use of confocal microscopy for nanoparticle drug delivery through skin. J Biomed Opt. 2013;18:061214.
35. Lopez RFV, Lange N, Guy RH, Bentley MVLB. Photodynamic therapy of skin cancer: controlled drug delivery of 5-ALA and its esters. Adv Drug Deliv Rev. 2004;56:77–94.
36. Araújo LMPC, Thomazine JA, Lopez RFV. Development of microemulsions to topically deliver 5-aminolevulinic acid in photodynamic therapy. Eur J Pharm Biopharm. 2010;75:48–55.
37. Casas A, Fukuda H, Di Venosa G, Batlle A. The influence of the vehicle on the synthesis of porphylins after topical application of 5-aminolaevulinic acid. Implications in cutaneous photodynamic sensitization. Br J Dermatol. 2000;143:564–72.
38. Valenta C, Auner BG, Loibl I. Skin permeation and stability studies of 5-aminolevulinic acid in a new gel and patch preparation. J Control Release. 2005;107:495–501.